

CurveCloudNet: Processing Point Clouds with 1D Structure

Colton Stearns
Stanford University

Jiateng Liu
Zhejiang University

Davis Rempe
Stanford University

Despoina Paschalidou
Stanford University

Jeong Joon Park
Stanford University

Sébastien Mascha
Summer Robotics

Leonidas J. Guibas
Stanford University

Abstract

Modern depth sensors such as LiDAR operate by sweeping laser-beams across the scene, resulting in a point cloud with notable 1D curve-like structures. In this work, we introduce a new point cloud processing scheme and backbone, called CurveCloudNet, which takes advantage of the curve-like structure inherent to these sensors. While existing backbones discard the rich 1D traversal patterns and rely on Euclidean operations, CurveCloudNet parameterizes the point cloud as a collection of polylines (dubbed a “curve cloud”), establishing a local surface-aware ordering on the points. Our method applies curve-specific operations to process the curve cloud, including a symmetric 1D convolution, a ball grouping for merging points along curves, and an efficient 1D farthest point sampling algorithm on curves. By combining these curve operations with existing point-based operations, CurveCloudNet is an efficient, scalable, and accurate backbone with low GPU memory requirements. Evaluations on the ShapeNet, Kortex, Audi Driving, and nuScenes datasets demonstrate that CurveCloudNet outperforms both point-based and sparse-voxel backbones in various segmentation settings, notably scaling better to large scenes than point-based alternatives while exhibiting better single object performance than sparse-voxel alternatives.

1. Introduction

Many modern 3D sensors such as LiDAR operate by sweeping laser-beams across the scene. As the laser traverses object surfaces, it returns dense measurements along the scanning direction, resulting in a 3D point cloud with notable curve-like structures (see Fig. 2). While the computer vision community has proposed various backbones for processing 3D point clouds for fundamental tasks such as semantic segmentation [38, 39, 51, 46, 20] and object detection [55, 50, 56, 58, 66], they rarely make use of the innate curve-like structures of the scanner outputs.

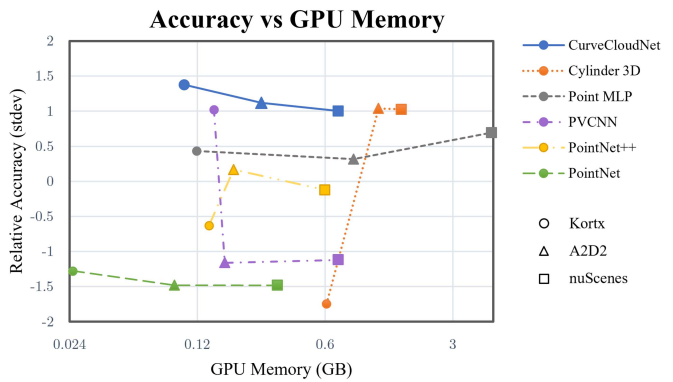


Figure 1: *Performance Comparison.* CurveCloudNet achieves high relative accuracy using low GPU memory. Unlike point and sparse-voxel baselines, our method performs well across both object (Kortex [1]) and scene-level (A2D2 [17], nuScenes [5]) datasets. Metrics are measured on an NVIDIA RTX3090 GPU.

In this work, we present a novel point cloud processing scheme designed to explicitly consider the curve-like structure of 3D sensor outputs. Instead of treating each point independently, we parameterize the point cloud as a collection of polylines, i.e. curves. As a result, we establish a local structure on the points, allowing for efficient communication between points along a curve. We propose a new backbone, CurveCloudNet, that applies 1D operations along curves. CurveCloudNet is efficient, scalable, and accurate, achieving state-of-the-art segmentation and classification performance on objects and large outdoor scenes with varying scanning patterns.

Existing backbones [39, 43, 21, 49, 64, 13, 57, 46] that directly operate on 3D points typically exchange and aggregate point features in Euclidean space, and have shown success on several downstream tasks (e.g. semantic segmentation, shape classification, etc.) for individual objects or relatively small indoor scenes. These methods, how-

ever, do not scale well to large scenes (e.g. in outdoor settings) due to inefficiencies in processing large unstructured point sets. On the other hand, recent voxel-based methods [53, 43, 18, 10, 31, 75, 20, 70] rely on efficient sparse data structures that scale better to large scenes. However, they require additional memory and, for small point sets, incur a latency overhead. Additionally, sensors with irregular and unpredictable sampling densities can lead to challenges in discretization, as previous works have noted in the case of fine structures [26] or cylindrical patterns [75].

Our proposed CurveCloudNet combines 1D curve reasoning with established point-based operations to achieve the best of both points and voxels. That is, curve reasoning makes our backbone scalable, accurate, and low-memory for both objects and large-scale scenes and across many scanning patterns. To the best of our knowledge, our work is the first to experimentally showcase accurate and efficient predictions on *both* object-level and outdoor datasets. The essence of CurveCloudNet is a novel adaptation of three standard point cloud operations for 1D curve structures: (1) a *symmetrical 1D convolution* that operates along curves, (2) a *ball grouping* similar to PointNet++ [39] that groups points along curves, and (3) an efficient *1D farthest-point-sampling* algorithm on curves. We integrate these components into our new architecture, combining curve operations with point-based operations [51, 39, 33, 20], resulting in a versatile, high-performing backbone that uses little GPU memory (see Fig. 1).

We evaluate CurveCloudNet on both object-level and outdoor scene-level datasets. For the object part segmentation task, we use ShapeNet [7, 69] along with our new Kortex [1] dataset; the latter includes real-world data of objects scanned in a curve-like manner. For the outdoor semantic segmentation task, we use the nuScenes [5] and Audi Autonomous Driving (A2D2) [17] datasets. The A2D2 dataset offers a unique sensor configuration resulting in a grid-like scanning pattern, which is distinct from previous LiDAR datasets [16, 5, 8, 44]. Supplementary experiments on object classification demonstrate flexibility to other perception tasks. Our evaluations demonstrate that using curve structures leads to improved performance on all experiments.

In summary, we make the following **contributions**: (1) we propose operating on laser-scanned point cloud data using a *curve cloud* representation, (2) we adapt common point cloud operations, including the ball grouping, convolution, and farthest point sampling, to efficiently run on curve clouds, (3) we design a novel backbone, CurveCloudNet, that makes use of both curve and point operations, and (4) we show state-of-the-art segmentation results on real-world data captured for both objects and large-scale scenes with various scanning patterns.

2. Related Work

Existing point cloud methods can be roughly characterized as point-based and voxel-based approaches. As our work addresses trade-offs between them, we discuss related works from each category.

Point-Based Networks. Prior work has extensively studied backbones that map a 3D point cloud to a high-dimensional feature space used for downstream applications, such as 3D reconstruction, shape classification, part segmentation, semantic segmentation, and more [14, 38, 39, 51, 46]. PointNet [38] was a seminal work that combined a series of MLPs with a max pooling layer to learn point-wise features. Following PointNet, several works proposed to aggregate local neighborhood information using hierarchical grouping at multiple geometric scales [39, 27, 40]. Recently, Ma et al. [33] introduced a compelling MLP-based architecture that combines residual multi-scale reasoning and affine transformations. Nevertheless, most hierarchical and MLP point networks are inefficient on large-scale point clouds, and although several backbones [20, 72, 68] have addressed this, they trade off scalability with task-specific frameworks or lower accuracy. In contrast, CurveCloudNet uses an efficient curve cloud representation to achieve superior performance on both objects and large-scale scenes.

Another line of research introduced *kernel-based convolutions* for learning per-point local features [43, 21, 49, 64, 13, 57, 26, 23, 24, 46, 52]. Kernels are defined using a family of polynomial functions [64] or can be estimated using MLPs [49, 30]. Likewise, [2, 46, 57, 63, 4] defined the kernel weights directly using the local 3D point coordinates. More related to our work is CurveNet [59], which proposed to perform random walks on point clouds and aggregate features along these “curves” to capture local geometric details. In contrast, our work defines efficient point cloud operations for existing 1D curve structures.

An alternative line of research proposed to construct a graph from the input point cloud and apply *graph-based convolutions* [45, 28, 9, 12] to capture local geometric structure. For example, [42] introduced a graph-based network that replaced convolutions with correlations computed between points and their k -nearest neighbors. Similarly, [48, 51] proposed to construct a local neighborhood graph and apply convolutional operations on the edges connecting neighboring pairs of points. Recent works [60, 29, 67, 71, 15, 74, 36] have also explored applying *attention-based aggregation* using transformer architectures with self-attention [47]. Unlike previous graph-based and attention-based networks, CurveCloudNet reasons over local 1D “curve” neighborhoods.

Voxel-Based Networks. Although point-based backbones can successfully process individual objects or small indoor scenes, they struggle to scale to large point clouds due to

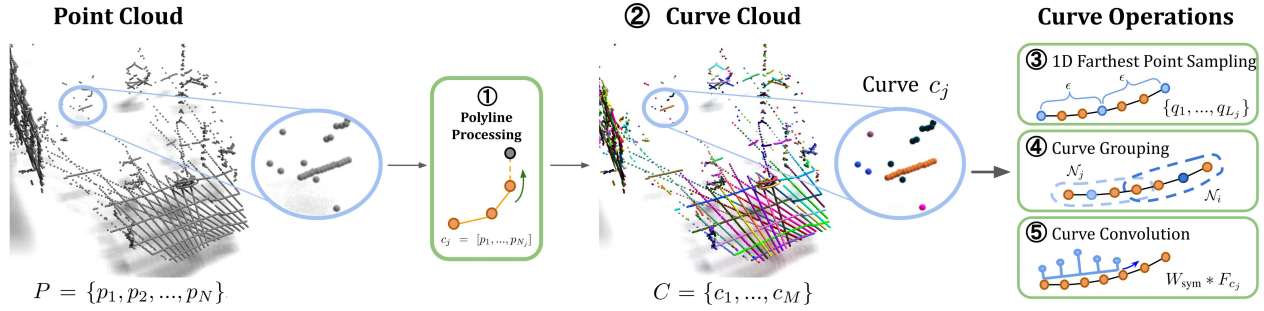


Figure 2: *Overview of Curve Cloud Reasoning.* Starting from laser-scanned input data, we ① link points into polylines to ② parameterize the point cloud as a curve cloud (see Sec. 3.1). We develop operations for learned architectures to specifically exploit the curve structure, including ③ 1D farthest-point-sampling along a curve, ④ curve grouping, and ⑤ symmetric curve convolutions (see Sec. 3.2).

inefficiency in processing large unstructured point sets. To address this, several works [43, 18, 10, 31, 73, 75, 70, 65, 25, 32, 62, 19] proposed to convert a point cloud into a 3D voxel grid and use this volumetric representation. Early works converted a point cloud into a dense voxel grid and applied dense 3D convolutions [34, 37], however the cubic size of the dense grid proved to be computationally prohibitive. PVCNN [31] was a seminal work in combining point operations with low-resolution dense voxel convolutions to efficiently process smaller-scale point clouds.

To scale to large scenes, several works [10, 25, 75, 32, 19] employed the sparse-voxel data structure from [18]. PVNAS [32] incorporated a network architecture search, demonstrating the importance of the architecture channels, network depth, kernel sizes, and training schedule. PVT [70] introduced a sparse attention module to efficiently process per-voxel local features using a transformer encoder [47]. Other methods seek a better voxel discretization of point clouds captured with LiDAR scans. For example, PolarNet [73] proposed to partition input points using grid cells defined in a polar coordinate system, while Cylinder3D [75] employed a cylindrical partitioning scheme based on a cylindrical coordinate system. In an alternative line of research, many methods [54, 61, 53, 57] employed spherical or bird’s-eye view projections to represent point clouds as images that are passed to a convolutional neural network.

Unlike these works, our model directly operates on points and curves, scaling to larger scenes without 2D or 3D convolutions. Furthermore, our model does not rely on the point cloud to exhibit cylindrical or planar properties.

3. Method: Learning on Curve Clouds

Our method takes as input a 3D point cloud, parses it into a curve cloud representation, and then processes the resulting curves for perception tasks by leveraging specialized curve operations, as shown in Fig. 2. We focus on object

part segmentation, semantic scene segmentation, and object classification, although in principle, our method is suitable for any other point cloud perception task.

3.1. Constructing Curve Clouds

Problem Formulation. The input to our model is the output of a laser-based 3D sensor represented as a point cloud $P = \{p_1, p_2, \dots, p_N\}$, where $p_i = [x_i, y_i, z_i]$ refers to the 3D coordinates of the i -th point. For each point, we are also given an associated acquisition timestamp t_i and an integer laser beam ID $b_i \in [1, B]$, which are readily available from sensors like LiDAR and are helpful in extracting curve information. For a scanner with B unique laser beams, b_i indicates which beam captured the point while t_i gives the ordering in which points were captured. Timestamps differ only by microseconds and indicate point ordering for constructing the curve cloud; otherwise, the point cloud is treated as an instantaneous capture of the scene.

We assume that each laser beam in the scanner captures 3D points *sequentially* and at a *high sampling rate* as it sweeps the scene. Concretely, if points $p_1, p_2,$ and p_3 are recorded consecutively by beam b , then their timestamps are ordered $t_1 < t_2 < t_3$. Moreover, if two consecutive points are spatially farther apart than some small threshold δ , we assume there is a surface discontinuity and the points lie on different surfaces in the scene.

Curve Clouds. A curve $c_j = [p_1, \dots, p_{N_j}]$ is defined as a sequence of N_j points where consecutive point pairs are connected by a line segment, i.e., a *polyline*. The curve is bi-directional and is equivalently defined as $c_j = [p_{N_j}, p_{N_j-1}, \dots, p_1]$. A *curve cloud* $C = \{c_1, \dots, c_M\}$ is an unordered set of M curves where each curve may contain a different number of points. Converting the input point cloud P to a corresponding curve cloud is straightforward and extremely efficient. Points from each beam b_i are ordered by timestamp and split into curves based on distances between consecutive points. If the distance between two consecu-

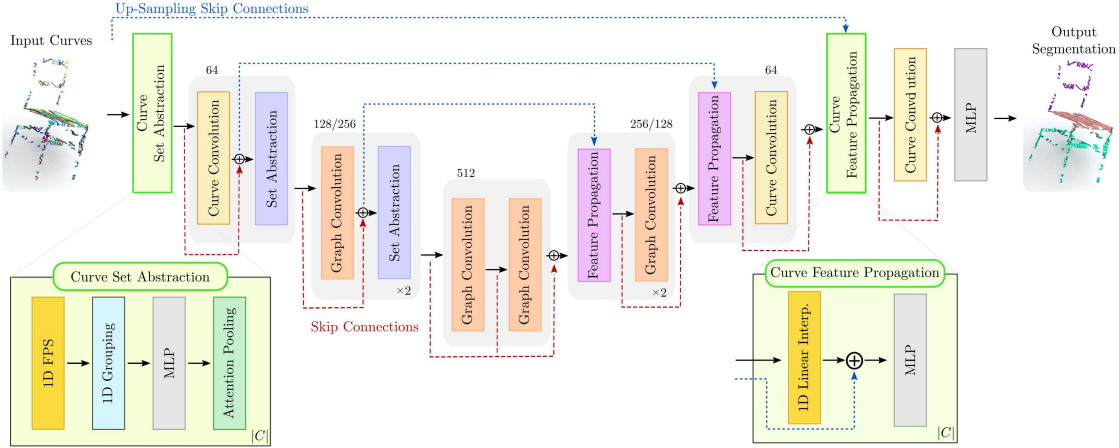


Figure 3: *CurveCloudNet Architecture*. The network employs a mix of curve and point layers to process a curve cloud through progressive down-sampling followed by up-sampling with skip connections. Curve layers operate on higher resolutions to efficiently capture the 1D structure, while at lower resolutions point layers propagate information across curves. Feature dimensions are listed above each block.

tive points is more than a set threshold δ while traversing the points in time order, then the current curve ends and a new curve begins, i.e., a surface discontinuity has occurred. In practice, we parallelize this process across all points and laser beams on the GPU. More details regarding the conversion process are provided in the supplement.

Why Use Curves? Curve clouds inherit the benefits associated with the 3D point cloud representation including lightweight data structures, low memory usage, and no need to discretize the space. But operating on curve clouds also has several advantages over point clouds. Point clouds are highly unstructured, making operations like nearest neighbor queries and convolutions expensive. Curve clouds add structure through point ordering along the polylines, allowing curves to be treated as 1D grids that enable constant-time neighborhood queries and efficient convolutions. This structure is flexible to any laser scanning pattern unlike, e.g., cylindrical voxel grids and polar range-view projections. In principle, the curve structure should also bring out the geometric properties of the surface it represents, such as surface curvature, tangents, and boundaries.

3.2. Operating on Curves

We now discuss the fundamental operations for curves. These operations are inspired by point cloud processing counterparts, so we start by reviewing operations on points.

3.2.1 Review of Point Cloud Layers

Our operations are based on those introduced in PointNet++ [39] and DGCNN [51]. In particular, these point-based methods rely heavily on *sampling*, *grouping*, *feature interpolation*, and *convolution* operations. We briefly re-

view the point layers relevant to these operations.

Set Abstraction (SA). Set abstraction is the downsampling layer introduced in [39]. It proceeds by (1) *sampling* a subset of “centroid” points from the point cloud at the current resolution, (2) *grouping* the points around these centroids into local neighborhoods, (3) translating points into the local frame of their centroid and processing all points with a shared MLP, and (4) pooling over each local neighborhood to get a downsampled point cloud with associated features. *Sampling* uses iterative farthest point sampling (FPS) [39]. *Grouping* commonly uses a ball query, which groups together all points within a specified radius from a centroid.

Feature Propagation (FP). Feature propagation is the up-sampling layer introduced in [39]. Its goal is to propagate features from a low-resolution point cloud $\{q_1, \dots, q_L\}$ with L points to a higher-resolution point cloud $\{p_1, \dots, p_H\}$ with H points where $L < H$. This is achieved with *feature interpolation*: given the low-res point features $\{g_1, \dots, g_L\}$, the high-res point features $F = \{f_1, \dots, f_H\}$ are determined by a distance-weighted feature interpolation of the k nearest low-res neighbors for each high-res point (based on the spatial coordinates of the points).

Graph Convolution. DGCNN [51] leverages convolution operations on a dynamically constructed graph to process points. At each layer, the graph is constructed by adding edges between each point and its k nearest neighbors in the learned feature space. The convolution centered at a point uses a learned edge function for each edge followed by aggregation. Constructing a dynamic graph in feature space is computationally prohibitive on larger scenes, so we opt to construct the graph based on 3D point distances (Sec. 3.3).

3.2.2 Curve Operations

We introduce new operations for *sampling*, *grouping*, *feature interpolation*, and *convolutions* along curves to expressively and efficiently learn on curve clouds.

1D Farthest Point Sampling. FPS is frequently a bottleneck in point cloud architectures and can be costly for large point clouds [20]. Subsampling L points from a point cloud of N points has a time complexity of $O(N^2)$ due to paired distance computations, and requires $O(L)$ sequential steps. For curves, we alleviate this cost with an approximation of FPS *along each curve* independently in a 1D manner. This amounts to sampling a subset of points on each curve that are evenly-spaced along the length of that curve (i.e., geodesically). For a curve c_j with N_j points, we subsample a point set $\{q_1, \dots, q_{L_j}\}$ with $L_j < N_j$ such that all pairs of contiguous points are about ϵ apart, where ϵ is a fixed target spacing shared across *all* curves. In other words, $d(q_i, q_{i-1}) \approx \epsilon$ for $i = 2, \dots, L_j$ where d measures the geodesic distance between two points along the same curve. Notably, this algorithm has only $O(N)$ complexity and can be parallelized across each curve independently.

Grouping Along Curves. After sampling, we must group points into local neighborhoods around the subsampled points on each curve. To do this, we adapt the previously discussed ball query to operate along each curve. For a query point p_i belonging to curve c_j (one of the “centroids” from sampling), we define the local neighborhood of p_i as $\mathcal{N}_i = \{p_k \in c_j \mid d(p_i, p_k) < r\}$ where r is a fixed neighborhood radius. In addition to being computationally faster than a standard 3D ball query grouping, using 1D curve groupings ensures that all neighborhoods lie on a continuous section of scanned surfaces.

Curve Feature Interpolation. To upsample on curves, we must interpolate features from a lower-resolution polyline to a higher-resolution one. Let p_h be the h^{th} point on the high-res curve, which falls between subsampled low-res points q_i and q_{i-1} with associated features g_i and g_{i-1} . The interpolated high-res feature f_h is simply the distance-weighted interpolation of the two low-res points.

Symmetric Curve Convolution. To process points along curves, we take advantage of expressive convolutions. However, it is computationally burdensome to compute point neighborhoods on the fly and run convolutions on unordered data [32]. Instead, we treat each curve as a discrete grid of features that can be convolved similar to a 1D image. To account for the bi-directionality of curves, we employ a symmetric convolution and thus produce equivalent results when applied “forward” or “backward” along the curve.

In particular, for a curve $c_j = [p_1, p_2, \dots, p_{N_j}]$ with associated point features $F_j = [f_1, f_2, \dots, f_{N_j}]$, we start by extracting additional features using the the L1 norm of feature gradients along the curve [52], denoted as $\nabla F_j =$

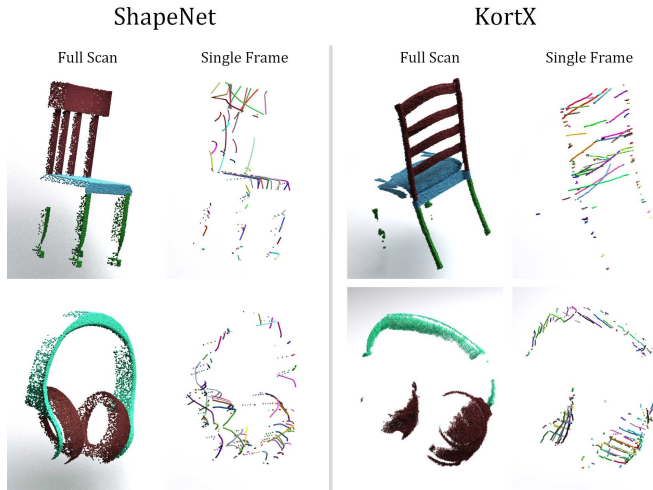


Figure 4: *Object Data Examples.* Simulated ShapeNet (left) and real-world Kortx (right) scans. The full (aggregated) scan and a single “frame” of 2048 point measurements are shown. Frame points depicted with the same color correspond to the same curve.

$[|\nabla f_1|, |\nabla f_2|, \dots, |\nabla f_{N_j}|]$. Note the norm is necessary to remove directional information. Concatenating these features together as $[F_j, \nabla F_j] \in \mathbb{R}^{N \times D}$ gives a grid on which to perform 1D convolutions. To respect bi-directionality, symmetric kernels are used for the convolution: for a kernel $W \in \mathbb{R}^{S \times D}$ with size S and D channels, we ensure $W_i = W_{S-i+1}$ for $i = 1, \dots, S$ where $W_i \in \mathbb{R}^D$.

3.2.3 Curve Layers

We integrate curve operations into curve layers that act as building blocks for the backbone detailed in Sec. 3.3.

Curve Set Abstraction (Curve SA). Curve set abstraction is a curve-centric downsampling procedure. For each curve, Curve SA (1) samples a subset of centroid points using *1D farthest point sampling*, (2) groups points along the curve using *curve grouping*, (3) translates points into the local frame of their centroid and processes them with a shared MLP, and (4) pools over each local neighborhood to get downsampled point features.

Curve Feature Propagation (Curve FP). Curve feature propagation is a curve-centric upsampling layer. For a curve c_j , its goal is to propagate features from a low-res polyline $[q_1, \dots, q_{L_j}]$ with L_j points to a higher-res polyline $[p_1, \dots, p_{H_j}]$ with H_j points where $L_j < H_j$. This is achieved using *curve feature interpolation* described above. Afterwards, the high-res interpolated features are concatenated with skip-linked features from a corresponding curve set abstraction layer and processed by a shared MLP.

Curve Convolution. The curve convolution layer allows for efficient communication and feature extraction along a

Method	ShapeNet	Kortx Dataset (\uparrow)							Kortx Performance (\downarrow)		
	mIOU (\uparrow)	mIOU	Cap	Chair	Earphone	Knife	Mug	Rocket	Time (ms)	GPU (GB)	Param (M)
PointNet [38]	63.1 \pm 0.4	68.5 \pm 1.8	77.1	80.1	62.5	62.9	56.0	72.4	10	0.29	1.49
PointNet++ [39]	66.9 \pm 1.2	71.0 \pm 2.5	69.3	65.9	83.1	70.4	71.7	65.5	109	1.95	1.53
DGCNN [51]	64.6 \pm 0.8	73.3 \pm 0.9	73.0	76.6	81.1	79.6	58.3	71.2	143	1.45	2.18
PointMLP [33]	72.1 \pm 0.4	75.4 \pm 1.3	77.2	75.3	78.8	83.1	64.6	73.6	58	0.83	16.76
PVCNN [31]	71.2 \pm 0.9	77.6 \pm 1.4	82.0	79.9	71.7	72.4	83.3	74.4	36	1.85	4.20
Cylinder3D [75]	58.6 \pm 0.5	63.5 \pm 0.2	64.8	56.9	80.8	55.1	64.8	58.7	96	5.76	56.03
CurveCloudNet	73.0 \pm 0.9	78.9 \pm 1.1	69.1	87.3	86.7	87.0	74.7	67.8	77	1.01	8.74

Table 1: *Object Segmentation Results.* Class-average mIOU is reported for synthetic ShapeNet and real-world Kortx data. CurveCloudNet achieves the highest accuracy compared to point and voxel baselines. Performance is on an Nvidia RTX 3090 GPU (batch size 16).

curve. This module consists of three sequential *symmetric curve convolutions*, each followed by batch normalization [22] and a leaky ReLU activation.

3.3. Curve Cloud Backbone: CurveCloudNet

We propose a novel architecture, CurveCloudNet, that processes curve clouds for several perception tasks. In Fig. 3, we illustrate CurveCloudNet as designed for segmentation tasks where the output is a single semantic class (one-hot vector) for each point in the input point cloud. Hence, it follows the U-Net [41] structure, consisting of a series of downsampling layers followed by upsampling with skip connections. Although in our experiments (Sec. 4) we focus on segmentation tasks, CurveCloudNet can be also adapted to other point cloud perception tasks from laser scanners (see supplement for a classification example).

Our architecture is a mix of curve and point-based layers. At higher resolutions, curve modules are employed since they are efficient and can capture geometric details when curve sampling is most dense across surfaces in the scene. At lower resolutions, point modules are used to propagate information across curves when 1D structure is less apparent. This combination makes CurveCloudNet an expressive network that maintains the benefits of point cloud backbones while injecting structure and efficiency usually only possible with voxel-based approaches.

Training. We train CurveCloudNet on segmentation tasks with a standard cross-entropy loss. Following previous works, we also supplement the loss with a Lovasz loss [3, 75] for nuScenes and Audi Autonomous Driving datasets. At training, we apply random scaling and translation augmentations, as well as random flips on nuScenes and Audi.

4. Experiments

CurveCloudNet achieves accurate and efficient prediction on both object-level and outdoor scene-level datasets (see Fig. 1). In Sec. 4.1 we evaluate our model on the task

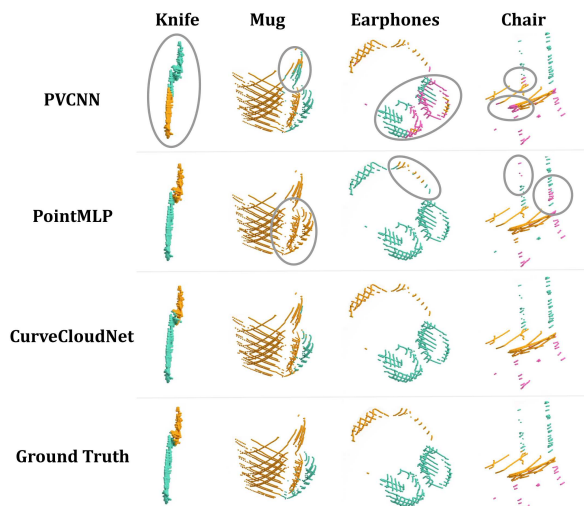


Figure 5: *Qualitative Results on Kortx.* Compared to point-based baselines, CurveCloudNet successfully segments fine-grained parts by leveraging curve structures.

of object-level part segmentation on ShapeNet [7] and on a new dataset collected with the Kortx vision system [1]. In Sec. 4.2 and Sec. 4.3, we evaluate semantic segmentation on larger outdoor scenes using the Audi Autonomous Driving Dataset (A2D2) [17] and nuScenes dataset [5], respectively. We note that each dataset exhibits a unique sensor scanning configuration. Sec. 4.4 ablates the key components of CurveCloudNet. For more experiments including classification, please refer to the supplementary material.

4.1. Object Part Segmentation

ShapeNet Dataset. The ShapeNet Part Segmentation Benchmark [6, 69] contains 16,881 synthetic shape models across 16 different categories. To match the Kortx dataset discussed below, we train and evaluate on only six categories: *cap*, *chair*, *earphone*, *knife*, *mug*, and *rocket*. Fol-

Method	Type	mIoU (\uparrow)	Performance (\downarrow)			Per-Class mIoU (\uparrow)												
			Time (ms)	GPU (GB)	Param (M)	car	bicycle	truck	person	road	sidewalk	obstacle	building	nature	pole	sign	signal	
PointNet [38]	Point-based	34.2	11	0.09	1.47	54.1	1.8	27.2	1.6	88.9	49.5	10.7	55.5	65.2	6.3	22.3	13.3	
PointNet++ [39]		46.5	53	0.19	1.52	62.4	9.3	55.7	3.6	90.3	58.0	12.7	79.3	82.1	19.2	36.6	48.7	
RandLANet [20]		43.4	16	0.05	1.24	60.2	4.8	46.7	7.5	91.3	57.2	14.9	78.9	80.0	16.6	27.7	34.3	
PointMLP [33]		47.6	63	0.86	16.8	65.8	9.8	54.2	15.8	92.5	63.5	14.8	81.7	82.9	18.8	34.6	36.9	
PVCNN [31]	Sparse-voxel	36.6	20	0.17	2.56	46.2	1.0	39.5	2.5	87.8	45.5	9.4	67.9	73.7	12.0	26.4	24.3	
Cylinder3D [75]		53.0	61	1.18	55.8	71.1	11.6	74.8	22.1	92.5	66.1	18.3	82.6	84.2	19.1	41.6	52.0	
CurveCloudNet	Curve	53.6	70	0.27	10.2	71.3	10.7	77.8	20.4	92.4	66.7	18.3	82.9	85.0	21.1	44.2	51.6	

Table 2: *A2D2 Segmentation Results*. On grid-like LiDAR scans, CurveCloudNet outperforms all other backbones in terms of mIoU and uses significantly less GPU memory and fewer parameters than Cylinder3D. Performance is on an Nvidia RTX 3090 GPU (batch size 1).

lowing the official splits [69], these categories yield 6,398 training shapes and 460 validation shapes. To evaluate performance on the laser-based scans that we are interested in, we simulate laser capture using the ShapeNet meshes. We randomly sample a sensor pose facing the mesh and a set of linear laser traversals, then sample points on the mesh along each traversal (see Fig. 4, left). For each training shape, we generate five synthetic scans from different sensor poses, yielding a training set of 31,991 point clouds.

Kortx Dataset. Kortx is a perception software system developed by Summer Robotics [1] that directly generates and operates on 3D curves sampled from a triangulated system of event sensors and laser scanners. Kortx software supports arbitrary continuous scan patterns, allowing a user to create their own patterns and use their own scan hardware. Using Kortx, we scan 7 real-world objects (cap, chair, earphone, knife, mug-1, mug-2, and rocket) multiple times in different poses, collecting 39 scans in total. Examples of scanned objects are provided in the right side of Fig. 4. Because the Kortx platform provides a continuous event-based 3D scan output (points are sampled every $5\mu\text{s}$), we defined a “frame” as a batch of 2048 consecutive point measurements, corresponding to roughly a 20Hz frame rate. Because each frame differs in its dynamic scanning pattern, we evaluate on 5 consecutive frames per scan in our Kortx dataset, hence resulting in 195 point clouds in total. We will release this dataset upon publication.

Results. We train CurveCloudNet and several baselines on the simulated ShapeNet training set and evaluate all methods on the simulated ShapeNet validation set and our Kortx dataset. All methods are trained over four random seeds, and we report the mean and standard deviation of the class-averaged mean intersection-over-union (mIoU) over the runs. For fair comparison, all models are trained for 60 epochs using the same hyperparameters, and the best validation mIoU throughout training is reported.

Results are summarized in Tab. 1. CurveCloudNet out-

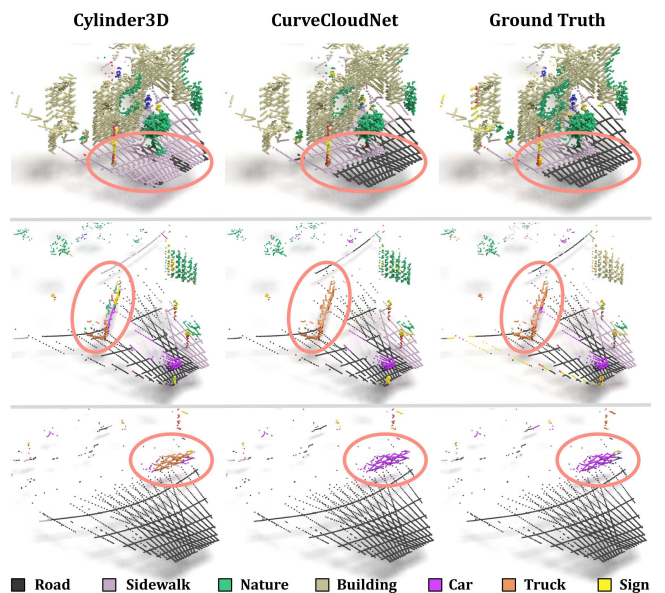


Figure 6: *Qualitative Results on A2D2*. Compared to Cylinder3D, CurveCloudNet can inform larger-object prediction with fine-grained details, e.g., identifying the curb of the sidewalk (top), cohesively segmenting all parts of a truck (middle), and distinguishing a car from a truck (bottom).

performs baselines on both datasets, effectively handling in-domain scans (ShapeNet) and generalizing to out-of-domain scans (Kortx). CurveCloudNet is competitive with other object-level backbones in terms of latency and GPU memory usage. In contrast, Cylinder3D, which is designed for large outdoor scenes, exhibits lower accuracy, worse latency, and higher GPU memory usage on this object-level task. Fig. 5 shows that CurveCloudNet distinguishes fine-grained structures, such as chair legs, mug handles, and the orientation of a near-symmetrical knife.

Method	Type	mIoU (\uparrow)	Performance (\downarrow)			Per-Class mIoU (\uparrow)															
			Time (ms)	GPU (GB)	Param (M)	barrier	bicycle	bus	car	construction	motorcycle	pedestrian	traffic cone	trailer	truck	driveable	other flat	sidewalk	terrain	manmade	vegetation
PointNet [38]	Point-based	21.5	15	0.33	1.5	16.6	0.0	23.1	33.0	1.5	0.0	4.8	10.3	4.4	14.2	76.2	14.0	22.0	35.2	41.5	46.5
PointNet++ [39]		51.1	274	0.60	1.5	60.1	6.5	58.4	66.3	16.4	20.0	50.8	12.6	31.5	42.0	94.0	60.8	63.8	69.2	82.4	82.3
RandLANet [20]		62.9	21	0.18	1.2	72.5	12.6	36.6	81.8	38.7	72.3	68.5	37.3	44.7	59.7	95.3	87.0	69.7	71.1	73.2	85.9
PointMLP [33]		67.9	164	4.94	16.8	72.3	27.8	88.2	86.3	37.2	51.0	60.7	50.6	56.4	71.1	95.7	70.6	70.9	72.0	88.8	87.2
RangeNet++* [35]	Range-view	65.5	-	-	-	66.0	21.3	77.2	80.9	30.2	66.8	69.6	52.1	54.2	72.3	94.1	66.6	63.5	70.1	83.1	79.8
Salsanext* [11]		72.2	-	-	-	74.8	34.1	85.9	88.4	42.2	72.4	72.2	63.1	61.3	76.5	96.0	70.8	71.2	71.5	86.7	84.4
PVCNN [31]	Sparse-voxel	29.4	29	0.71	2.6	42.1	3.4	37.4	57.9	8.7	2.6	12.6	9.1	30.1	33.2	90.1	54.9	51.4	59.7	70.4	66.7
PolarNet* [73]		71.0	-	-	-	74.7	28.2	85.3	90.9	35.1	77.5	71.3	58.8	57.4	76.1	96.5	71.1	74.7	74.0	87.3	85.7
Cylinder3D* [75]		76.1	80	1.57	55.9	76.4	40.3	91.2	93.8	51.3	78.0	78.9	64.9	62.1	84.4	96.8	71.6	76.4	75.4	90.5	87.4
CurveCloudNet	Curve	75.6	146	0.71	8.9	76.7	42.4	92.1	90.5	46.0	79.1	79.1	63.3	62.0	80.5	96.8	72.0	75.8	75.6	89.4	88.3

Table 3: *nuScenes Segmentation Results*. On typical sweeping LiDAR scans, CurveCloudNet scales significantly better than other point-based backbones and is competitive with Cylinder3D. Performance is on an Nvidia RTX 3090 GPU (batch size 1). * indicates that results are copied from the referenced papers.

4.2. A2D2 LiDAR Segmentation

A2D2 Dataset. The Audi Autonomous Driving Dataset (A2D2) [17] contains 41,280 frames of outdoor driving scenes captured from 5 overlapping LiDAR sensors, creating a unique grid-like scanning pattern (see Fig. 2). Each frame is annotated from the front-facing camera with a 38-category semantic label. To the best of our knowledge, we are the first to evaluate LiDAR segmentation on this relatively new dataset, so we pre-process the data for our setup. We define a mapping from camera categories to LiDAR categories and remove texture-only (e.g. sky, lane markers, blurred-area) and very rare categories (e.g. animals, tractors, utility vehicles). In total, we evaluate on 12 LiDAR categories: *car*, *bicycle*, *truck*, *person*, *road*, *sidewalk*, *obstacle*, *building*, *nature*, *pole*, *sign*, and *traffic signal*. Evaluation is constrained to annotated LiDAR points, i.e. the field of view of the front-facing camera.

Results. We train CurveCloudNet along with point and voxel-based baselines on the official A2D2 training split [17]. For fair comparison, all models are trained for 140 epochs using the same hyperparameters, and the best validation mIOU throughout training is reported.

Results are summarized in Tab. 2. CurveCloudNet scales to outdoor scenes significantly better than point-based backbones, with the runner-up PointMLP showing 6% drop in mIOU and a 3 \times increase in GPU memory. Compared to the voxel-based backbone Cylinder3D [75], CurveCloudNet achieves higher accuracy with similar latency and a 4 \times reduction in GPU memory, which is beneficial for on-board autonomous vehicle (AV) applications. The strong performance on the grid-like sampling pattern of A2D2 suggests that CurveCloudNet is well-suited for more general LiDAR data that does not follow a uniform sweeping pattern. Fig. 6 qualitatively demonstrates the potential advan-

tage of CurveCloudNet over Cylinder3D.

4.3. nuScenes LiDAR Segmentation

nuScenes Dataset. The nuScenes dataset [5] contains 1000 sequences of driving data, each 20 seconds long. Each sequence contains 32-beam LiDAR data with segmentations annotated at 2Hz. We follow the official nuScenes benchmark protocol with 16 semantic categories.

Results. We train CurveCloudNet and the baselines on the official nuScenes training split. To ensure fair comparison, we train all models for 100 epochs. Results on the nuScenes validation split are shown in Tab. 3. CurveCloudNet significantly improves upon other point-based networks: PointMLP shows more than a 7% drop in mIOU and $\sim 7\times$ increase in GPU memory. CurveCloudNet also outperforms projection-based methods RangeNet++ [35] and Salsanext [11], and achieves comparable accuracy to the voxel-based Cylinder3D while using half the GPU memory. Overall, CurveCloudNet bridges the gap between point and voxel-based methods: it scales point-based processing to large outdoor scenes, achieving competitive accuracy to voxel-based methods. Furthermore, CurveCloudNet’s small memory footprint makes it suitable for on-board AV applications and mobile devices.

4.4. Ablation Study

Tab. 4 shows an ablation analysis of CurveCloudNet on the A2D2 dataset; the table shows that each of our proposed curve operations is essential to achieve high accuracy and efficiency. We ablate grouping along curves by instead using the regular radial groupings from PointNet++ [39]. This ignores the curve structure and results in decreased accuracy, increased latency, and a significant increase in GPU memory usage. Instead of curve farthest point sampling, we

Curve Operations			Performance (\downarrow)			
Grouping	FPS	1D Conv.	mIoU (\uparrow)	Time (ms)	GPU (GB)	Param (M)
✓	✓	✓	53.6	70	0.27	10.3
✗	✓	✓	53.3	99	1.03	10.3
✓	✗	✓	52.4	105	0.26	10.3
✓	✓	✗	52.0	61	0.20	9.9
✗	✗	✗	52.6	122	0.92	10.3

Table 4: *Ablation Study on A2D2*. Curve operations are ablated and replaced with the standard point-based counterparts.

also try regular FPS, which causes a decreased accuracy and increased latency. Finally, without 1D curve convolutions, we observe a notable decline in accuracy with a marginal improvement in latency and GPU memory. Taken together, our curve operations increase accuracy with roughly half the latency and one third the GPU memory requirements.

5. Discussion

We have described a point-processing backbone, CurveCloudNet, which introduces curve-level operations to achieve efficient, versatile, and accurate performance on 3D perception tasks. CurveCloudNet shows state-of-the-art results on the ShapeNet, Kortex, nuScenes, and A2D2 datasets, exhibiting a trade-off between accuracy and memory budgets as well as a unified solution to *both* small and large-scale scenes with various scanning patterns.

In future research, we intend to incorporate explicit curve-to-curve communication that can further improve accuracy and efficiency on large scenes. Additionally, we believe an exciting direction will be to explicitly incorporate geometric properties of polylines, such as surface tangents and normals along with their connectivity via intersections.

References

- [1] Summer robotics. <https://www.summerrobotics.ai/>. Accessed: 2023-02-15. 1, 2, 6, 7
- [2] Matan Atzmon, Haggai Maron, and Yaron Lipman. Point convolutional neural networks by extension operators. *ACM Trans. on Graphics*, 2018. 2
- [3] Maxim Berman, Amal Rannen Triki, and Matthew B. Blaschko. The lovász-softmax loss: A tractable surrogate for the optimization of the intersection-over-union measure in neural networks. In *Proc. IEEE Conf. on Computer Vision and Pattern Recognition (CVPR)*, 2018. 6
- [4] Alexandre Boulch, Gilles Puy, and Renaud Marlet. Fkaconv: Feature-kernel alignment for point cloud convolution. 2020. 2
- [5] Holger Caesar, Varun Bankiti, Alex H Lang, Sourabh Vora, Venice Erin Liong, Qiang Xu, Anush Krishnan, Yu Pan, Giancarlo Baldan, and Oscar Beijbom. nuscenes: A multi-modal dataset for autonomous driving. 2020. 1, 2, 6, 8
- [6] Angel X. Chang, Thomas Funkhouser, Leonidas Guibas, Pat Hanrahan, Qixing Huang, Zimo Li, Silvio Savarese, Manolis Savva, Shuran Song, Hao Su, Jianxiong Xiao, Li Yi, and Fisher Yu. ShapeNet: An Information-Rich 3D Model Repository. Technical Report arXiv:1512.03012 [cs.GR], Stanford University — Princeton University — Toyota Technological Institute at Chicago, 2015. 6
- [7] Angel X. Chang, Thomas A. Funkhouser, Leonidas J. Guibas, Pat Hanrahan, Qi-Xing Huang, Zimo Li, Silvio Savarese, Manolis Savva, Shuran Song, Hao Su, Jianxiong Xiao, Li Yi, and Fisher Yu. Shapenet: An information-rich 3d model repository. *arXiv.org*, 1512.03012, 2015. 2, 6
- [8] Ming-Fang Chang, John Lambert, Patsorn Sangkloy, Jagjeet Singh, Slawomir Bak, Andrew Hartnett, De Wang, Peter Carr, Simon Lucey, Deva Ramanan, and James Hays. Argoverse: 3d tracking and forecasting with rich maps. In *IEEE Conference on Computer Vision and Pattern Recognition, CVPR 2019, Long Beach, CA, USA, June 16-20, 2019*, pages 8748–8757. Computer Vision Foundation / IEEE, 2019. 2
- [9] Jintai Chen, Biwen Lei, Qingyu Song, Haochao Ying, Danny Z. Chen, and Jian Wu. A hierarchical graph network for 3d object detection on point clouds. In *Proc. IEEE Conf. on Computer Vision and Pattern Recognition (CVPR)*, 2020. 2
- [10] Christopher B. Choy, JunYoung Gwak, and Silvio Savarese. 4d spatio-temporal convnets: Minkowski convolutional neural networks. In *Proc. IEEE Conf. on Computer Vision and Pattern Recognition (CVPR)*, 2019. 2, 3
- [11] Tiago Cortinhal, George Tzelepis, and Eren Erdal Aksoy. Salsanext: Fast, uncertainty-aware semantic segmentation of lidar point clouds. In *Proc. of the International Symposium on Advances in Visual Computing (ISVC)*, 2020. 8
- [12] Moshe Eliasof and Eran Treister. Diffgen: Graph convolutional networks via differential operators and algebraic multigrid pooling. In *Advances in Neural Information Processing Systems (NeurIPS)*, 2020. 2
- [13] Carlos Esteves, Christine Allen-Blanchette, Ameesh Makadia, and Kostas Daniilidis. Learning SO(3) equivariant representations with spherical cnns. In *Proc. of the European Conf. on Computer Vision (ECCV)*, 2018. 1, 2
- [14] Haoqiang Fan, Hao Su, and Leonidas J. Guibas. A point set generation network for 3d object reconstruction from a single image. *Proc. IEEE Conf. on Computer Vision and Pattern Recognition (CVPR)*, 2017. 2
- [15] Hehe Fan, Yi Yang, and Mohan Kankanhalli. Point 4d transformer networks for spatio-temporal modeling in point cloud videos. In *Proc. IEEE Conf. on Computer Vision and Pattern Recognition (CVPR)*, 2021. 2
- [16] Andreas Geiger, Philip Lenz, and Raquel Urtasun. Are we ready for autonomous driving? The KITTI vision benchmark suite. In *Proc. IEEE Conf. on Computer Vision and Pattern Recognition (CVPR)*, 2012. 2
- [17] Jakob Geyer, Yohannes Kassahun, Mentar Mahmudi, Xavier Ricou, Rupesh Durgesh, Andrew S. Chung, Lorenz Hauswald, Viet Hoang Pham, Maximilian Mühlegg, Sebastian Dorn, Tiffany Fernandez, Martin Jänicke, Sudesh Mirashi, Chiragkumar Savani, Martin Sturm, Oleksandr Vorobiov, Martin Oelker, Sebastian Garreis, and Peter Schuberth.

- A2D2: audi autonomous driving dataset. *arXiv.org*, 2020. [1](#), [2](#), [6](#), [8](#)
- [18] Benjamin Graham, Martin Engelcke, and Laurens van der Maaten. 3d semantic segmentation with submanifold sparse convolutional networks. In *Proc. IEEE Conf. on Computer Vision and Pattern Recognition (CVPR)*, 2018. [2](#), [3](#)
- [19] Yuenan Hou, Xinge Zhu, Yuexin Ma, Chen Change Loy, and Yikang Li. Point-to-voxel knowledge distillation for lidar semantic segmentation. *2022 IEEE/CVF Conference on Computer Vision and Pattern Recognition (CVPR)*, pages 8469–8478, 2022. [3](#)
- [20] Qingyong Hu, Bo Yang, Linhai Xie, Stefano Rosa, Yulan Guo, Zhihua Wang, Niki Trigoni, and Andrew Markham. Randla-net: Efficient semantic segmentation of large-scale point clouds. In *Proc. IEEE Conf. on Computer Vision and Pattern Recognition (CVPR)*, 2020. [1](#), [2](#), [5](#), [7](#), [8](#)
- [21] Binh-Son Hua, Minh-Khoi Tran, and Sai-Kit Yeung. Point-wise convolutional neural networks. In *Proc. IEEE Conf. on Computer Vision and Pattern Recognition (CVPR)*, 2018. [1](#), [2](#)
- [22] Sergey Ioffe and Christian Szegedy. Batch normalization: Accelerating deep network training by reducing internal covariate shift. pages 448–456, 2015. [6](#)
- [23] Artem Komarichev, Zichun Zhong, and Jing Hua. A-CNN: annularly convolutional neural networks on point clouds. In *Proc. IEEE Conf. on Computer Vision and Pattern Recognition (CVPR)*, 2019. [2](#)
- [24] Shiyi Lan, Ruichi Yu, Gang Yu, and Larry S Davis. Modeling local geometric structure of 3d point clouds using geocnn. In *Proc. IEEE Conf. on Computer Vision and Pattern Recognition (CVPR)*, 2019. [2](#)
- [25] Alex H. Lang, Sourabh Vora, Holger Caesar, Lubing Zhou, Jiong Yang, and Oscar Beijbom. Pointpillars: Fast encoders for object detection from point clouds. *2019 IEEE/CVF Conference on Computer Vision and Pattern Recognition (CVPR)*, pages 12689–12697, 2018. [3](#)
- [26] Huan Lei, Naveed Akhtar, and Ajmal Mian. Octree guided CNN with spherical kernels for 3d point clouds. In *Proc. IEEE Conf. on Computer Vision and Pattern Recognition (CVPR)*, 2019. [2](#)
- [27] Jiaxin Li, Ben M Chen, and Gim Hee Lee. So-net: Self-organizing network for point cloud analysis. In *Proc. IEEE Conf. on Computer Vision and Pattern Recognition (CVPR)*, 2018. [2](#)
- [28] Jinxian Liu, Bingbing Ni, Caiyuan Li, Jiancheng Yang, and Qi Tian. Dynamic points agglomeration for hierarchical point sets learning. In *Proc. of the IEEE International Conf. on Computer Vision (ICCV)*, 2019. [2](#)
- [29] Xinhai Liu, Zhizhong Han, Yu-Shen Liu, and Matthias Zwicker. Point2sequence: Learning the shape representation of 3d point clouds with an attention-based sequence to sequence network. In *Proceedings of the AAAI conference on artificial intelligence*, 2019. [2](#)
- [30] Yongcheng Liu, Bin Fan, Shiming Xiang, and Chunhong Pan. Relation-shape convolutional neural network for point cloud analysis. In *Proc. IEEE Conf. on Computer Vision and Pattern Recognition (CVPR)*, 2019. [2](#)
- [31] Zhijian Liu, Haotian Tang, Yujun Lin, and Song Han. Point-voxel CNN for efficient 3d deep learning. In *Advances in Neural Information Processing Systems (NeurIPS)*, 2019. [2](#), [3](#), [6](#), [7](#), [8](#)
- [32] Zhijian Liu, Haotian Tang, Shengyu Zhao, Kevin Shao, and Song Han. Pvnas: 3d neural architecture search with point-voxel convolution. *IEEE Transactions on Pattern Analysis and Machine Intelligence*, 44:8552–8568, 2021. [3](#), [5](#)
- [33] Xu Ma, Can Qin, Haoxuan You, Haoxi Ran, and Yun Fu. Rethinking network design and local geometry in point cloud: A simple residual mlp framework. In *Proc. of the International Conf. on Learning Representations (ICLR)*, 2022. [2](#), [6](#), [7](#), [8](#)
- [34] Daniel Maturana and Sebastian Scherer. Voxnet: A 3d convolutional neural network for real-time object recognition. In *Proc. IEEE International Conf. on Intelligent Robots and Systems (IROS)*, 2015. [3](#)
- [35] Andres Milioto, Ignacio Vizzo, Jens Behley, and Cyrill Stachniss. Rangenet ++: Fast and accurate lidar semantic segmentation. In *Proc. IEEE International Conf. on Intelligent Robots and Systems (IROS)*, 2019. [8](#)
- [36] Ishan Misra, Rohit Girdhar, and Armand Joulin. An end-to-end transformer model for 3d object detection. In *Proc. of the IEEE International Conf. on Computer Vision (ICCV)*, 2021. [2](#)
- [37] C. Qi, Hao Su, Matthias Nießner, Angela Dai, Mengyuan Yan, and Leonidas J. Guibas. Volumetric and multi-view cnns for object classification on 3d data. *2016 IEEE Conference on Computer Vision and Pattern Recognition (CVPR)*, pages 5648–5656, 2016. [3](#)
- [38] Charles R Qi, Hao Su, Kaichun Mo, and Leonidas J Guibas. Pointnet: Deep learning on point sets for 3d classification and segmentation. In *Proc. IEEE Conf. on Computer Vision and Pattern Recognition (CVPR)*, 2017. [1](#), [2](#), [6](#), [7](#), [8](#)
- [39] Charles R Qi, Li Yi, Hao Su, and Leonidas J Guibas. Pointnet++: Deep hierarchical feature learning on point sets in a metric space. In *Advances in Neural Information Processing Systems (NIPS)*, 2017. [1](#), [2](#), [4](#), [6](#), [7](#), [8](#)
- [40] Gordon Guocheng Qian, Yuchen Li, Houwen Peng, Jinjie Mai, Hasan Abed Al Kader Hammoud, Mohamed Elhoseiny, and Bernard Ghanem. Pointnext: Revisiting pointnet++ with improved training and scaling strategies. *ArXiv*, abs/2206.04670, 2022. [2](#)
- [41] Olaf Ronneberger, Philipp Fischer, and Thomas Brox. U-net: Convolutional networks for biomedical image segmentation. In *Medical Image Computing and Computer-Assisted Intervention (MICCAI)*, 2015. [6](#)
- [42] Yiru Shen, Chen Feng, Yaoqing Yang, and Dong Tian. Mining point cloud local structures by kernel correlation and graph pooling. In *Proc. IEEE Conf. on Computer Vision and Pattern Recognition (CVPR)*, 2018. [2](#)
- [43] Hang Su, Varun Jampani, Deqing Sun, Subhransu Maji, Evangelos Kalogerakis, Ming-Hsuan Yang, and Jan Kautz. Splatnet: Sparse lattice networks for point cloud processing. In *Proc. IEEE Conf. on Computer Vision and Pattern Recognition (CVPR)*, 2018. [1](#), [2](#), [3](#)
- [44] Pei Sun, Henrik Kretschmar, Xerxes Dotiwalla, Aurelien Chouard, Vijaysai Patnaik, Paul Tsui, James Guo, Yin Zhou,

- Yuning Chai, Benjamin Caine, Vijay Vasudevan, Wei Han, Jiquan Ngiam, Hang Zhao, Aleksei Timofeev, Scott Etinger, Maxim Krivokon, Amy Gao, Aditya Joshi, Yu Zhang, Jonathon Shlens, Zhifeng Chen, and Dragomir Anguelov. Scalability in perception for autonomous driving: Waymo open dataset. In *2020 IEEE/CVF Conference on Computer Vision and Pattern Recognition, CVPR 2020, Seattle, WA, USA, June 13-19, 2020*, pages 2443–2451. Computer Vision Foundation / IEEE, 2020. 2
- [45] Gusi Te, Wei Hu, Amin Zheng, and Zongming Guo. RGCNN: regularized graph CNN for point cloud segmentation. In *ACM Trans. on Graphics*, 2018. 2
- [46] Hugues Thomas, Charles R. Qi, Jean-Emmanuel Deschaud, Beatriz Marcotequi, François Goulette, and Leonidas J. Guibas. Kpconv: Flexible and deformable convolution for point clouds. In *Proc. of the IEEE International Conf. on Computer Vision (ICCV)*, 2019. 1, 2
- [47] Ashish Vaswani, Noam Shazeer, Niki Parmar, Jakob Uszkoreit, Llion Jones, Aidan N. Gomez, Lukasz Kaiser, and Illia Polosukhin. Attention is all you need. In *Advances in Neural Information Processing Systems (NIPS)*, pages 5998–6008, 2017. 2, 3
- [48] Nitika Verma, Edmond Boyer, and Jakob Verbeek. Featnet: Feature-steered graph convolutions for 3d shape analysis. In *Proc. IEEE Conf. on Computer Vision and Pattern Recognition (CVPR)*, 2018. 2
- [49] Shenlong Wang, Simon Suo, Wei-Chiu Ma, Andrei Pokrovsky, and Raquel Urtasun. Deep parametric continuous convolutional neural networks. In *Proc. IEEE Conf. on Computer Vision and Pattern Recognition (CVPR)*, June 2018. 1, 2
- [50] Yue Wang and Justin M. Solomon. Object DGCNN: 3d object detection using dynamic graphs. In *Advances in Neural Information Processing Systems (NeurIPS)*, 2021. 1
- [51] Yue Wang, Yongbin Sun, Ziwei Liu, Sanjay E. Sarma, Michael M. Bronstein, and Justin M. Solomon. Dynamic graph CNN for learning on point clouds. *ACM Trans. on Graphics*, 2019. 1, 2, 4, 6
- [52] Ruben Wiersma, Ahmad Nasikun, Elmar Eisemann, and Klaus Hildebrandt. Deltaconv: anisotropic operators for geometric deep learning on point clouds. *ACM Trans. on Graphics*, 2022. 2, 5
- [53] Bichen Wu, Alvin Wan, Xiangyu Yue, and Kurt Keutzer. SqueezeSeg: Convolutional neural nets with recurrent CRF for real-time road-object segmentation from 3d lidar point cloud. In *Proc. IEEE International Conf. on Robotics and Automation (ICRA)*, 2018. 2, 3
- [54] Bichen Wu, Xuanyu Zhou, Sicheng Zhao, Xiangyu Yue, and Kurt Keutzer. SqueezeSegv2: Improved model structure and unsupervised domain adaptation for road-object segmentation from a lidar point cloud. In *Proc. IEEE International Conf. on Robotics and Automation (ICRA)*, 2019. 3
- [55] Hai Wu, Jinhao Deng, Chenglu Wen, Xin Li, Cheng Wang, and Jonathan Li. Casa: A cascade attention network for 3-d object detection from lidar point clouds. *IEEE Trans. Geosci. Remote. Sens.*, 2022. 1
- [56] Hai Wu, Chenglu Wen, Wei Li, Xin Li, Ruigang Yang, and Cheng Wang. Transformation-equivariant 3d object detection for autonomous driving. *arXiv.org*, 2022. 1
- [57] Wenxuan Wu, Zhongang Qi, and Fuxin Li. Pointconv: Deep convolutional networks on 3d point clouds. In *Proc. IEEE Conf. on Computer Vision and Pattern Recognition (CVPR)*, 2019. 1, 2, 3
- [58] Xiaopei Wu, Liang Peng, Honghui Yang, Liang Xie, Chenxi Huang, Chengqi Deng, Haifeng Liu, and Deng Cai. Sparse fuse dense: Towards high quality 3d detection with depth completion. In *Proc. IEEE Conf. on Computer Vision and Pattern Recognition (CVPR)*, 2022. 1
- [59] Tiange Xiang, Chaoyi Zhang, Yang Song, Jianhui Yu, and Weidong Cai. Walk in the cloud: Learning curves for point clouds shape analysis. In *Proc. of the IEEE International Conf. on Computer Vision (ICCV)*, 2021. 2
- [60] Saining Xie, Sainan Liu, Zeyu Chen, and Zhuowen Tu. Attentional shapecontextnet for point cloud recognition. In *Proc. IEEE Conf. on Computer Vision and Pattern Recognition (CVPR)*, 2018. 2
- [61] Chenfeng Xu, Bichen Wu, Zining Wang, Wei Zhan, Peter Vajda, Kurt Keutzer, and Masayoshi Tomizuka. SqueezeSegv3: Spatially-adaptive convolution for efficient point-cloud segmentation. In *Proc. of the European Conf. on Computer Vision (ECCV)*, 2020. 3
- [62] Jianyun Xu, Ruixiang Zhang, Jian Dou, Yushi Zhu, Jie Sun, and Shiliang Pu. Rpvnet: A deep and efficient range-point-voxel fusion network for lidar point cloud segmentation. In *Proc. of the IEEE International Conf. on Computer Vision (ICCV)*, 2021. 3
- [63] Mutian Xu, Runyu Ding, Hengshuang Zhao, and Xiaojuan Qi. Paconv: Position adaptive convolution with dynamic kernel assembling on point clouds. 2021. 2
- [64] Yifan Xu, Tianqi Fan, Mingye Xu, Long Zeng, and Yu Qiao. Spidercnn: Deep learning on point sets with parameterized convolutional filters. In *Proc. of the European Conf. on Computer Vision (ECCV)*, 2018. 1, 2
- [65] Yan Yan, Yuxing Mao, and Bo Li. Second: Sparsely embedded convolutional detection. *Sensors*, 2018. 3
- [66] Bangbang Yang, Chong Bao, Junyi Zeng, Hujun Bao, Yinda Zhang, Zhaopeng Cui, and Guofeng Zhang. Neumesh: Learning disentangled neural mesh-based implicit field for geometry and texture editing. In *Proc. of the European Conf. on Computer Vision (ECCV)*, 2022. 1
- [67] Jiancheng Yang, Qiang Zhang, Bingbing Ni, Linguo Li, Jinxian Liu, Mengdie Zhou, and Qi Tian. Modeling point clouds with self-attention and gumbel subset sampling. In *Proc. IEEE Conf. on Computer Vision and Pattern Recognition (CVPR)*, 2019. 2
- [68] Zetong Yang, Yanan Sun, Shu Liu, and Jiaya Jia. 3dssd: Point-based 3d single stage object detector. *2020 IEEE/CVF Conference on Computer Vision and Pattern Recognition (CVPR)*, pages 11037–11045, 2020. 2
- [69] Li Yi, Vladimir G Kim, Duygu Ceylan, I-Chao Shen, Mengyan Yan, Hao Su, Cewu Lu, Qixing Huang, Alla Sheffer, and Leonidas Guibas. A scalable active framework for region annotation in 3d shape collections. *ACM Transactions on Graphics (ToG)*, 2016. 2, 6, 7

- [70] Cheng Zhang, Haocheng Wan, Xinyi Shen, and Zizhao Wu. Pvt: Point-voxel transformer for point cloud learning. *arXiv.org*, 2022. [2](#), [3](#)
- [71] Wenxiao Zhang and Chunxia Xiao. PCAN: 3d attention map learning using contextual information for point cloud based retrieval. In *Proc. IEEE Conf. on Computer Vision and Pattern Recognition (CVPR)*, 2019. [2](#)
- [72] Yifan Zhang, Qingyong Hu, Guoquan Xu, Yanxin Ma, Jianwei Wan, and Yulan Guo. Not all points are equal: Learning highly efficient point-based detectors for 3d lidar point clouds. In *Proc. IEEE Conf. on Computer Vision and Pattern Recognition (CVPR)*, 2022. [2](#)
- [73] Yang Zhang, Zixiang Zhou, Philip David, Xiangyu Yue, Zerong Xi, Boqing Gong, and Hassan Foroosh. Polarnet: An improved grid representation for online lidar point clouds semantic segmentation. In *Proc. IEEE Conf. on Computer Vision and Pattern Recognition (CVPR)*, 2020. [3](#), [8](#)
- [74] Hengshuang Zhao, Li Jiang, Jiaya Jia, Philip H. S. Torr, and Vladlen Koltun. Point transformer. In *Proc. of the IEEE International Conf. on Computer Vision (ICCV)*, 2021. [2](#)
- [75] Hui Zhou, Xinge Zhu, Xiao Song, Yuexin Ma, Zhe Wang, Hongsheng Li, and Dahua Lin. Cylinder3d: An effective 3d framework for driving-scene lidar semantic segmentation. *arXiv.org*, 2020. [2](#), [3](#), [6](#), [7](#), [8](#)